ACEMP 2001
Kusadasi, June 2001

New Electric Reluctance Motor with Bulk Superconducting Materials on the Rotor

A. Leão Rodrigues

Department of Electrical Engineering
Faculty of Science and Technology
New University of Lisbon
2825-114 Caparica **PORTUGAL**
Email: leao@uninova.pt Tel: +351 212948545 Fax: +351 21294 8532

Abstract

The computer modelling, using the Finite Element Method (FEM), of reluctance machines with rotors containing both iron and High Temperature Superconducting (HTS) materials is presented in this paper. The modelling solves for field and stator current distribution from were reluctance torque is evaluated. The experimental results on a 2 kW reluctance motor using HTS materials on the rotor and cooled by liquid nitrogen, show that a torque of up 70% than that of a correspondent conventional machine can be attained. Pre-magnetisation of these rotors by field cooling is explained and this process gives a mechanical output power 4 to 5 times better than that of a conventional reluctance machine.

1 Introduction

Conventional reluctance motor theory is nowadays very well known [1]. Due to the simple rotor construction, robustness and easy winding commutation by means power electronic circuits (inverters), reluctance motors have today a large industrial application. The main disadvantage is to exhibit much less output torque than the equivalent salient pole synchronous motor.
During the last two decades many different reluctance rotor configurations have been considered in order to improve output power and efficiency of these motors [2]. Recently, a number of international research groups [3] have explored the possibility of using High Temperature Superconducting (HTS) materials in the construction of electrical machines and in the particular of reluctance motors in order to increase their specific output power. In this way, smaller and lighter motors can replace their conventional counterparts. This is very important for applications such as in vehicles and in space where weight and volume are to be kept at a minimum. When cooled below their critical temperature T_c, superconductors can carry large current densities without any dissipation. In addition these materials have important magnetic properties.
Heike Kammerlingh Onnes discovered the superconductivity in 1911 in the mercury when cooled at 4.2 K. Many other elements and alloys exhibiting Superconductivity were afterwards discovered. However, the critical temperature T_c was below 23 K and therefore the superconductor had to be cooled by liquid helium (a Greek word for sun). Liquid helium cooling is expensive and this is the reason why superconductivity found until then only a few engineering applications.
This situation was modified in 1986, when Bednorz and Müller [4] discovered superconductivity in a copper oxide based ceramic with a perovskite structure at 35 K, a much higher temperature than any metallic superconductor of 1st generation. This discovery was rapidly followed by the identification of other based ceramic structures. One of the best of these perovskite structures is yttrium-barium-copper oxide (known as YBCO) discovered by P. Chu at the University of Huston, with a critical temperature T_c of 94 K. This discovery was particularly significant because that compound could be cooled with cheap and readily available liquid nitrogen. The ceramic YBCO is a type-II High Temperature Superconductor (HTS), or superconductor of 2nd generation, and can transport current densities higher than the standard copper wire (roughly 10 A/mm^2).
Large currents can therefore be realised in small superconductors without any dissipation and prohibitive cooling requirements and consequently scale down in size of the device using these materials.
The great disadvantage of the HTS materials in the construction of power devices is its brittle nature and thus the difficulty to be machined. When using HTS materials in electric motors much care must be taken in the design of the rotors in order to eliminate mechanical stresses in these fragile materials. Perhaps, reluctance rotors are the best candidates to employ these materials in their construction and different configurations, giving different torques, are now considered.

2 The reluctance torque of a conventional motor

Figure 1 shows the distribution of the flux density produced by the stator in a conventional reluctance motor when the rotor position is θ, obtained by means a commercial Finite Element package [5]. The salient type rotor rotating around the stator modulates the

magnetic circuit permeance $\mathscr{P}(\theta)$ according to the rotor position θ. Consequently, the stator winding inductance $L(\theta) = n^2\mathscr{P}(\theta)$ of the stator winding with n turns varies with rotor position. When the rotor longitudinal axis is aligned with the stator magnetic axis (θ = 0), the permeance is a maximum and therefore the stator inductance attains the maximum

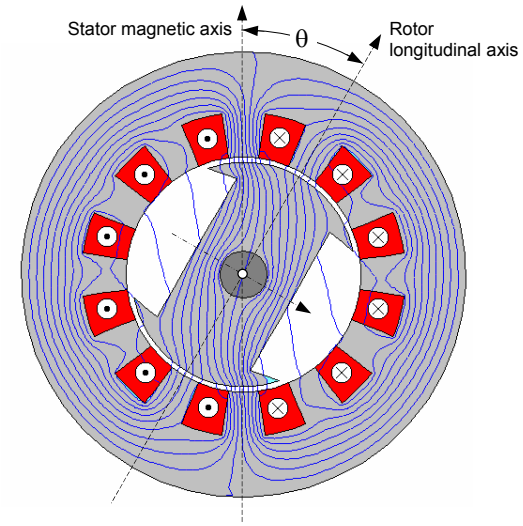

Fig. 1 – Flux plot for conventional reluctance motor

value L_{max}. On the other hand, when the rotor transversal axis is in the quadrature with the stator magnetic axis ($\theta = 90\ ^0Elect$), the stator inductance attains the minimum value L_{min}. For any rotor position θ of the longitudinal axis during a complete rotor revolution, and assuming sinusoidal variation for the magnetic circuit permeance, the sator inductance versus rotor position $L(\theta)$ can be written as

$$L(\theta) = \frac{1}{2}(L_{max} + L_{min}) + \frac{1}{2}(L_{max} - L_{min})\cos 2\theta \qquad (1)$$

as shown plotted in figure 2a.

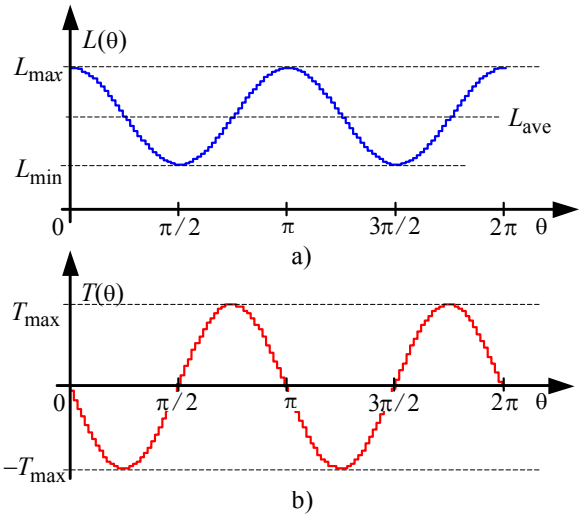

Fig. 2 – Inductance and torque variation versus rotor position in a conventional reluctance motor

The reluctance torque developed on the rotor shaft of this device with a constant r.m.s. current I through a single coil device is given, according to the reference [2], by the relation $T(\theta) = (1/2)I^2 dL(\theta)/d\theta$. For the three-phase reluctance motor case, substitution of (1) into (2) gives

$$T(\theta) = \frac{3}{2}I^2(L_{max} - L_{min})\sin(2\theta) \qquad (2)$$

For a three phase reluctance motor fed with a constant r.m.s. voltage and frequency $\omega = 2\pi f$, (2) takes the form

$$T(\theta) = \frac{3}{2}\frac{U^2}{\omega^2 L_{max}L_{min}}(L_{max} - L_{min})\sin(2\theta). \qquad (3)$$

Eqs. (2) and (3) show that the developed torque for the operation of a three-phase reluctance motor both with constant r.m.s. current or voltage versus θ have a similar variation. Reluctance torque increases with the increasing difference $(L_{max} - L_{min})$.

As shown plotted in figure 2b, the reluctance torque describes two cycles in one rotor revolution. The maximum torque value is attained for rotor positions $\theta = (k+1)\,90\ ^oElect.$ where $k = 0,1,2,\ldots$

3 Superconducting reluctance motor model

During recent years many different reluctance rotor configurations have been considered in order to optimise the difference $(L_{max} - L_{min})$. In conventional reluctance machines, this difference is amplified by increasing the transversal axis reluctance by flanking the rotor with flux barriers.

A novel possibility for increasing this difference is to use bulk HTS blocks on the rotor. The diamagnetic properties of superconductors make them ideal for this purpose.

Incorporating iron and superconducting materials on the rotor is possible to increase the flux along the longitudinal axis and almost shield it along the transversal axis and therefore optimising the reluctance torque. Two different rotor configurations can now be considered.

3.1 Salient type rotor configuration

The salient type reluctance motor incorporating two YBCO blocks glued, or placed in a grove, in each side of the rotor is shown in figure 3. The two superconducting blocks are electrically isolated and because of their diamagnetic nature they prevent transverse rotor flux to circulate. As a result, the value of L_{max} is maintained but the value of L_{min}

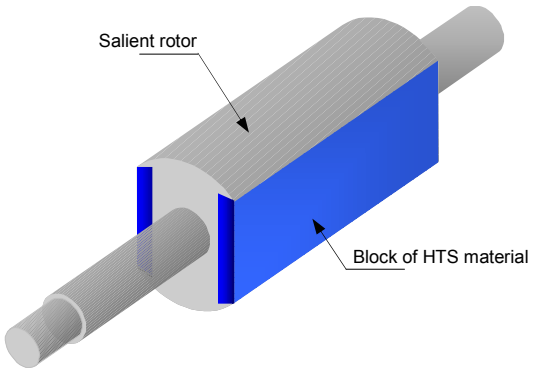

Fig. 3 – Salient type HTS rotor layout

decreases drastically. Figure 4 shows the flux plot produced by the stator winding. Comparing this result with that displayed in figure 1, it can be observed that the leakage flux is very small. Leakage flux is almost shielded due to the induced currents $+J_c$ and $-J_c$ that circulate axially in each HTS block.

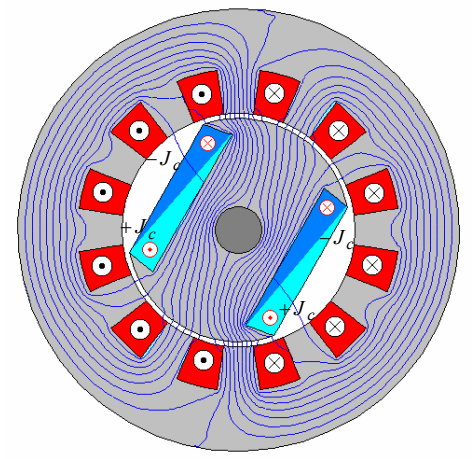

Fig. 4 – HTS salient rotor flux plot

The salient HTS type rotor has a simple construction and provides good start up performances. However, they can still be improved using other sophisticated rotor configuration as follows.

3.2 Composite type rotor configuration

Another possible configuration is the composite type rotor. Slices of iron and superconducting ceramics are assembled as shown in figure 5. Slices of YBCO or Bi-Ag elements can be used and a strong and balanced rotor is obtained. Again, the flux has a easy path along the longitudinal axis and a great reluctance along the transversal axis which results also in a considerable difference $L_{max}-L_{min}$ and consequently a high torque is produced. Figure 6 shows the flux plot produced by the stator winding in the composite rotor. It can be seen that, as in the case of salient type, transport currents $+J_c$ and $-J_c$ are circulating axially in each block, which penetrate about half of the ratio of the rotor [6].

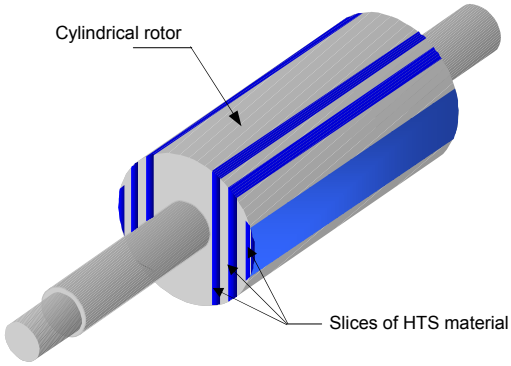

Fig. 5 – HTS composite rotor layout

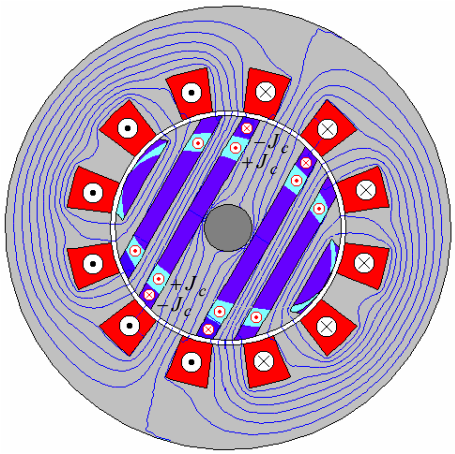

Fig. 6 – HTS composite rotor flux plot

The optimal torque is obtained when the iron and HTS plates have both the same thickness. However, due to the shaft the middle iron block is thicker.

4 Novel HTS rotor

In the previous configurations, the flux penetration into the HTS material is small and the current distribution is confined to a surface layer, leaving a large volume of the superconducting material inactive. The rotor can trap magnetic flux by utilizing more of the superconducting material. This can be achieved by electrically connected the two blocks of superconducting material forming a coil of one single turn, as shown in figure 7. In this case super currents can circulate the iron rotor and forming surrounding loops $+J_c$ and $-J_c$, like a field winding, as shown plotted in figure 8. In this case the rotor behaves as the best-known permanent magnet for the same equivalent volume of the superconductor. The output torque has now the reluctance component $T_R = A\sin 2\theta$ and an excitation synchronous torque

component $T_E = B\sin\theta$, giving a high resulting torque $T = A\sin 2\theta + B\sin\theta$. Because the synchronous or excitation torque is usual much greater than reluctance torque, the resulting torque variation has now one cycle per rotor revolution.

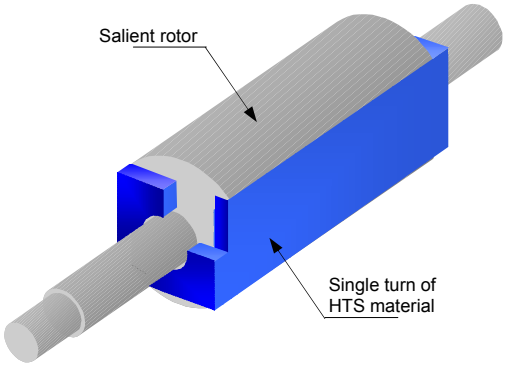

Fig. 7 – HTS forming a coil of one turn around the salient rotor

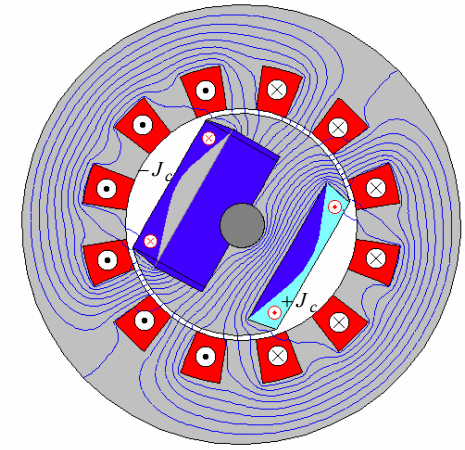

Fig. 8 – Rotor flux plot of the pre-magnetised rotor

The stator winding can be used to pre-magnetise the superconductor by field cooling. It is important that the pre-magnetising field penetrates further than the rotating field, otherwise, during the normal operation the trapped field can be lost [7]. Figure 9 illustrates the sequence of the HTS coil pre-magnetisation. With the ceramic material in the normal state, $T > T_c$, a static stator field is switched on. A flux density of about twice of the flux during normal operation is desirable. The second step is to cool the rotor with liquid nitrogen at temperature $T < T_c$ and maintaining the stator field. The superconductor will trap the flux. Finally, the stator current is switched off and super currents are induced in the superconductor penetrating further in the material. Therefore the rotor retains some trapped flux as a permanent magnet. The situation is maintained while the HTS material of the rotor is kept with a temperature $T < T_c$.

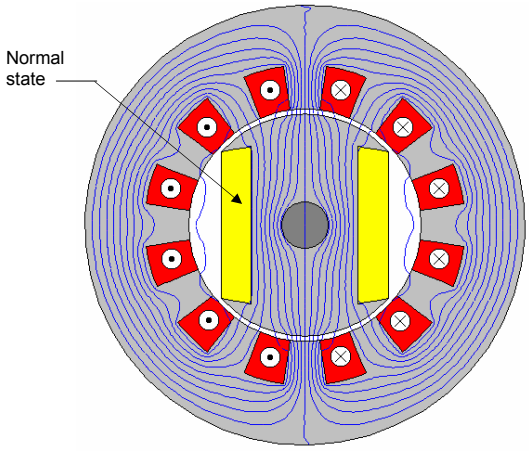

a) Stator current on and $T > T_c$

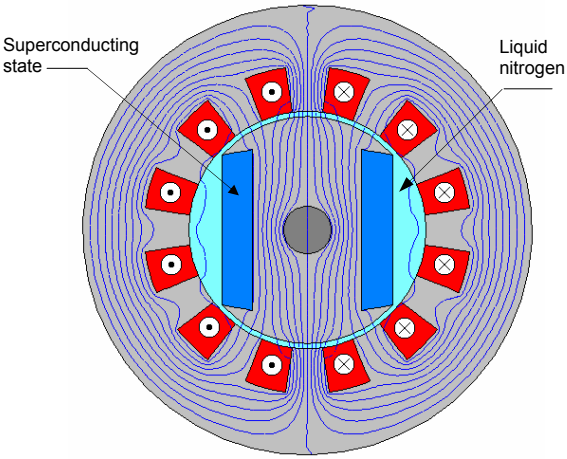

b) Stator current on and $T < T_c$

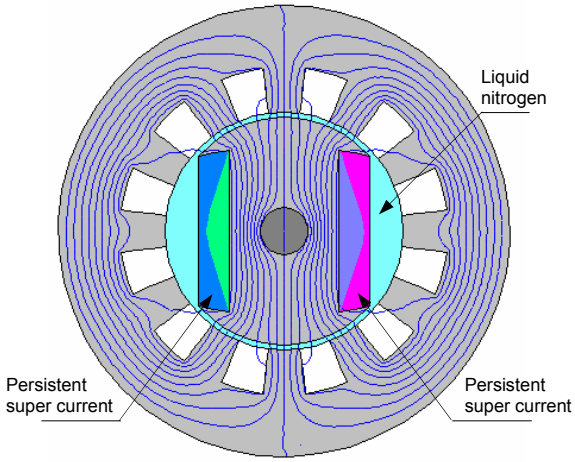

c) Stator current off and $T < T_c$

Fig. 9 – Pre-magnetisation of the synchronous motor by exciting and cooling the HTS material

5 Experimental results

A comparison of the salient, composite and pre magnetised synchronous developed torques by the previous machines, relative to the conventional reluctance torque is shown in figure 10.
The theoretical results show that the torque produced by the HTS *salient type motor* is about 1.7 times greater than the torque produced by the conventional motor and the HTS *composite type*, with five iron blocks and six YBCO blocks on the rotor, is about 2.2 times greater, but the construction is more complicated and expensive than that of salient pole.
However, the total torque $T = T_R + T_E$ developed in the *pre-magnetised rotor* is 3.7 times greater than the correspondent conventional reluctance torque. In figure 11 is shown the experimental results of the output power obtained from the four different rotors and identical 2 kW three-phase stator. These results are in a good agreement with those obtained by Kovalev [8].

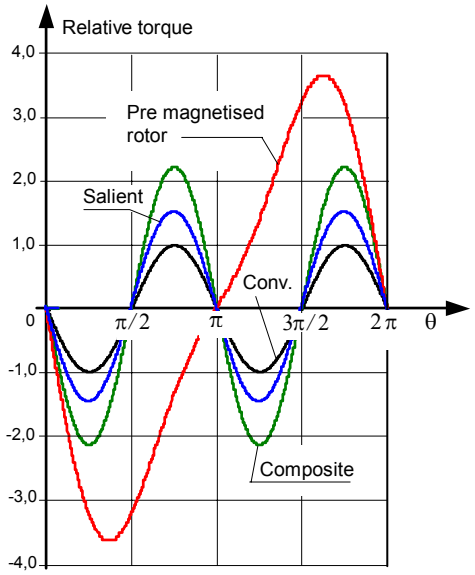

Fig. 10 – Relative developed torque comparison

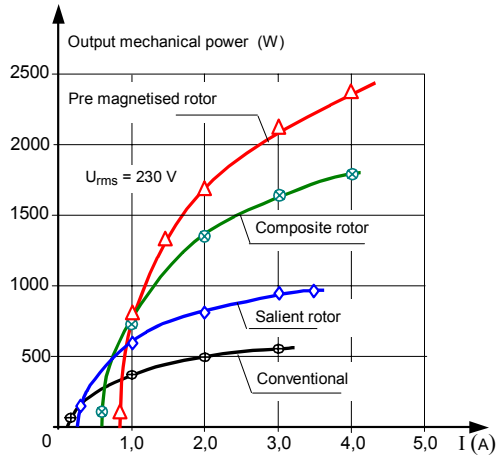

Fig. 11 – Output mechanical power comparison

6 Conclusions

Prediction of output power in HTS reluctance machines incorporating superconducting materials on the rotor was evaluated using a computer model. It was shown that considerable increasing in performance of the salient pole machine can be achieved by using blocks of superconductor materials working as flux shielding and sources of magnetisation. Better machines can be built using rotor pre-magnetisation.
However, in order to obtain these performances the rotor must be cooled under the critical temperature of the superconductor. Nevertheless, in locals where installations of liquid nitrogen or liquid hydrogen are available, such as in the near future hydrogen powered aircrafts (cryoplanes) and other land vehicles, where weight is undesirable, these type of motors can be serious competitors of conventional motors.

References

[1] - Miller T. J. E., *Switched Reluctance Motors and their Control*, Oxford Science Publications, 1993.

[2] - Match L. W. et al, *Electromagnetic and Electromechanical Machines*, Wiley & Sons, 1986.

[3] - Department Engineering Science University of Oxford, U.K.; Moscow State Aviation Institute, Moscow, Russia; Institut fuer Physikalische Hochtechnologie, Jena,Germany; Institute de Ciencia de Materials de Barcelona, Bellaterra, Spain; DEE-FCT/UNL, Caparica, Portugal.

[4] - Bednorz J.G., Müller K. A. *Z. Phys.* B 64 189.

[5] - Magnet 6.0, Infolytica Lda, Oxford.

[6] - Barnes G. J., McCulloch M., Dew-Hughes D. *Computational modelling of electric motors containing bulk type-II superconducting materials in the rotor,* Inst. Phys. Conf. Ser. Nº.167 (IPO Publishing Ltd) 1075-1078, 2000.

[7] - Barnes G. J., *Computational modelling for type-II superconductivity and the investigation of high temperature superconducting electrical machines*, Ph.D. Thesis, Oxford Univ.,2000.

[8] - Kovalev L. K.et al, *Theoretical and experimen-tal study of magnetisation and hysteresis process in single grain YBCO sphere and bulk melt textured YBCO ceramics*, Seminar on High Temperature Superconductivity, Jena, German, September 22-25, 1999.

* * *